JOURNAL OF GEOPHYSICAL RESEARCH, VOL. 113, A07102, doi:10.1029/2007JA012955, 2008

Forbush decreases of cosmic rays: Energy dependence of the recovery phase

I. G. Usoskin,[1] I. Braun,[2] O. G. Gladysheva,[3] J. R. Hörandel,[4] T. Jämsén,[1] G. A. Kovaltsov,[3] and S. A. Starodubtsev[5]

Received 26 November 2007; revised 18 February 2008; accepted 26 February 2008; published 16 July 2008.

[1] Cause and general shape of Forbush decreases of cosmic rays are relatively well understood, however, the knowledge of their recovery times remains rather poor. Earlier results of theoretical and fragmentary statistical studies are in disagreement whether the recovery time does or does not depend on the energy of cosmic rays. A thorough empirical study of the recovery phase of strong isolated Forbush decreases is presented here, based on the ground based data from the World Neutron Monitor Network since 1964 and three ground based muon telescopes since 1973. In total 39 strong Forbush decreases, suitable for the analysis, have been identified for the period 1964–2006, 24 of them depicting a clear energy dependence of the recovery time and 15 consistent with no energy dependence. All analyzed Forbush decreases with magnitudes exceeding 10% demonstrate an energy dependence of the recovery time, while smaller events can be of either type. No apparent relation between the occurrence of energy dependent/independent recovery and the IMF polarity has been found. This result provides an observational constraint for more detailed modeling of the propagation of interplanetary transients and their dynamic effects on cosmic ray transport.

Citation: Usoskin, I. G., I. Braun, O. G. Gladysheva, J. R. Hörandel, T. Jämsén, G. A. Kovaltsov, and S. A. Starodubtsev (2008), Forbush decreases of cosmic rays: Energy dependence of the recovery phase, *J. Geophys. Res.*, *113*, A07102, doi:10.1029/2007JA012955.

1. Introduction

[2] A Forbush decrease (FD) is a transient depression in the galactic cosmic ray (CR) intensity. Only classical Forbush decreases (e.g., recent review by *Cane* [2000], and references therein) are considered here, whereas other CR suppressions such as isolated magnetic clouds or recurrent events are beyond the present analysis. FDs are typically characterized by a sudden onset (often with a complicated time structure) reaching a minimum within about a day, followed by a more gradual recovery phase typically lasting from several days up to a few weeks. The magnitudes of FDs vary from a few percent up to 25% in the neutron monitor energy range. FDs are usually caused by transient interplanetary events, which are related to coronal mass ejections and shocks.

[3] Despite numerous publications related to the magnitude and general shape of a FD [see *Wibberenz et al.*, 1998; *Cane*, 2000, and references therein], studies of the FD recovery time and its energy dependence are quite limited. A classical analysis of FDs observed by ground-based neutron monitors (NMs) during 1957–1983 has been performed by *Lockwood et al.* [1986], who concluded that the recovery time does not depend on the energy of cosmic ray particles. On the other hand, earlier studies of FDs observed by both NMs and ground-based muon detectors [e.g., *Sandström and Forbush*, 1958; *Lockwood*, 1960; *Webber*, 1962; *Östman*, 1968, 1969] suggest that the recovery time of a FD is shorter for more energetic particles. A similar result has been obtained recently by *Jämsén et al.* [2007] who found a clear energy dependence of the recovery time for some FDs in 2004–2005. We are not aware of other systematic analysis of the energy dependence of FD recovery time including observations after 1983. A recent empirical study of the dependence of the FD recovery time on the parameters of interplanetary disturbances [*Penna and Quillen*, 2005] is based on data from a single NM and thus gives no information on the energy dependence.

[4] Theoretical predictions for the recovery phase are also controversial. The recovery time is predicted to be independent on the energy of CR particles because it mainly depends on the decay of interplanetary disturbance and only secondly on the transport parameters of particles [e.g., *Lockwood et al.*, 1986; *le Roux and Potgieter*, 1991; *Wibberenz et al.*, 1998]. However, *Mulder and Moraal* [1986] have shown, using the superposed epoch analysis, that the FD recovery time is related to the interplanetary

[1]Sodankylä Geophysical Observatory (Oulu Unit), University of Oulu, Oulu, Finland.
[2]Max-Planck-Institut für Kernphysik, Heidelberg, Germany.
[3]Ioffe Physical-Technical Institute, St. Petersburg, Russia.
[4]Department of Astrophysics, Radboud University Nijmegen, Netherlands.
[5]Yu.G. Shafer Institute of Cosmophysical Research and Aeronomy SB RAS, Yakutsk, Russia.

0148-0227/08/2007JA012955$09.00

Table 1. Muon Detectors Included in This Analysis

Telescope	Operation Range	Location	P_c, GV
YMT	1973–2003	Yakutsk, Russia	1.6
MUG	2003–2006	Pyhäsalmi, Finland	0.9
KMD	1993–2006	Karlsruhe, Germany	4

magnetic field (IMF) polarity. This result has been confirmed later by *Rana et al.* [1996] and *Singh and Badruddin* [2006]. The dependence of the recovery time on the polarity is related to the drift of CR particles in the heliosphere, which implicitly depends on their energy. This gives a hint at a possible relation between the particle's energy and the FD recovery time. We note that earlier studies were statistically limited as they were based on analyses of data on a limited number of FDs from a few detectors.

[5] Thus the question of the recovery rate of FDs is still open and a comprehensive empirical investigation of the energy (in)dependence of the recovery time is required. Here we present results of a thorough study of the FD recovery time for all major FDs (that satisfy the selection criteria presented in section 2.1) for the period 1964–2006, using all the available data from the neutron monitor (NM) network as well as from three ground-level muon telescopes (MTs).

2. Data and Method

2.1. Data and Selection Criteria

[6] The data analyzed here were recorded in the period 1964–2006, when data from the large world-wide network of neutron monitors are available. The hourly pressure corrected count rates of all the NMs recording the selected events have been obtained from the WDCCR database (http://www.env.sci.ibaraki.ac.jp/database/html/WDCCR/index.html). In addition to the NM database we use also data from three ground based muon telescopes listed in Table 1: the Yakutsk Muon Telescope in Russia, Muon Under-Ground detector in Pyhäsalmi, Finland, and Karlsruhe Muon Detector in Germany. Note that while YMT and MUG data are corrected only for the barometric pressure and may contain unaccounted trends and variations due to the changing atmospheric profile, KMD data are corrected also for the actual atmospheric density profile, measured semidiurnally on meteo-balloons, and are thus more robust. To take into account effects of muon production and decay in the atmosphere, the KMD data are annually corrected for their dependence on the ground pressure and the altitude of the 150 hPa layer in the atmosphere in an iterative procedure.

[7] Data containing long gaps (longer than one day), apparent errors (e.g., jumps due to snow effects in NM or atmospheric changes in MT data) or apparent trends during the period under investigation have been removed from further analysis.

[8] For the analysis we have selected only those FDs which satisfy the following criteria.

[9] 1. Only strong FDs with the magnitude $\langle M \rangle$ (see the definition in section 2.4) of 4% or higher were considered.

[10] 2. Only FDs with a clear recovery phase, which is not distorted by another transient event, were considered. Events with GLE (Ground Level Enhancement of cosmic rays) occurring during the recovery phase were not rejected but the entire day of the GLE occurrence was removed from the analysis (see comments in Table 3).

[11] 3. Only FDs where the recovery phase can be reasonably well approximated by an exponential shape (see section 2.3) were included. Records of individual detectors for each event were subject to an additional consistency test (see section 2.4) and rejected from further analysis if failing.

[12] Following these criteria, the 39 FDs listed in Tables 2 and 3 have been selected for further analysis. They are depicted in Figure 1 together with the time profile of CR intensity recorded by the Oulu NM. FDs can be seen in the Figure as sharp vertical dips in the count rate. Most of the selected FDs occurred around the maximum and declining phases of the solar cycle since strong FDs are rare during

Table 2. Parameters of the Forbush Decrease Recovery Time Analysis: The Start of the Recovery (Columns 1–2); the Database Used for the Analysis (3); the Mean Magnitude $\langle M \rangle$ (4) and the Mean Recovery Time $\langle \tau \rangle$ (5); the Energy Dependence of the Recovery Time α (6) and the Time Interval Used for the Analysis T (7)[a]

Events			Parameters		Results	
Year	Date	Database	$\langle M \rangle$ %	$\langle \tau \rangle$ (days)	$\alpha \pm \sigma_\alpha$, GeV^{-1}	T[b], days
			Events of Type I			
1966	4 Sep	48 NM	8.6	5.7	0.003 ± 0.025	11
1969	15 May	51 NM	7.4	6	0.016 ± 0.13	10
1969	3 Nov	47 NM	6.5	3.6	0 ± 0.015	11
1974	17 Sep	45 NM	7	4.9	−0.013 ± 0.056	10
1978	10 Mar	34 NM	8.6	4.9	−0.004 ± 0.02	12
1979	6 Apr	36 NM	5.5	3.9	−0.003 ± 0.02	11
1979	21 Sep	41 NM + YMT	9.5	7.1	0.008 ± 0.015	15(10)
1981	26 Jul	37 NM + YMT	7.3	2.7	0.003 ± 0.011	9(5)
1985	29 Apr	39 NM + YMT	5.6	6.3	0.003 ± 0.01	17
1999	14 Dec	30 NM + KMD	4	2.2	−0.037 ± 0.03	7(6)
2000	15 Aug	32 NM + YMT + KMD	4.7	2.7	0.002 ± 0.012	11(9)
2000	29 Nov	30 NM + KMD	7.8	7.5	−0.006 ± 0.024	22(8)
2001	13 Apr	36 NM + YMT	7	3	−0.004 ± 0.015	13(6)
2001	25 Nov	31 NM + YMT	7	1.8	0.003 ± 0.005	9(8)
2003	1 Jun	33 NM	7	2	−0.008 ± 0.011	9

[a]See text (section 2.4) for definition.
[b]Interval for the MT data is shown in parentheses if different from NM data.

Table 3. Continuation of Table 2

		Events of Type II				
1968	3 Nov	53 NM	9.1	2.9	0.009 ± 0.006	8
1970	10 Mar	44 NM	5.7	3.3	0.026 ± 0.01	10
1972	5 Aug	52 NM	13	3.8	0.023 ± 0.02	13
1972	2 Nov	51 NM	8.8	3.6	0.016 ± 0.012	11
1976	2 Apr	43 NM	5.8	2.9	0.029 ± 0.006	9
1978	2 May[a]	39 NM + YMT	19.9	6.2	0.015 ± 0.003	13(11)
1981	19 May	39 NM + YMT	12.2	6.3	0.03 ± 0.01	13(5)
1982	14 Jul	41 NM	23	8.5	0.027 ± 0.016	15
1984	28 Apr	37 NM	5	3.8	0.028 ± 0.009	12
1989	14 Mar[b]	40 NM + YMT	16.1	9.2	0.027 ± 0.013	15(11)
1991	13 Jun[c]	42 NM + YMT	22	5.5	0.01 ± 0.01	13(12)
1992	10 May	34 NM + YMT	12	4.5	0.019 ± 0.01	11(9)
1998	05 May	33 NM + YMT + KMD	5.6	4.5	0.029 ± 0.013	11(9)
1998	27 Aug	34 NM	10	4.3	0.013 ± 0.007	12
2000	9 Jun	32 NM + YMT	9.9	6.9	0.024 ± 0.011	11(9)
2000	16 Jul	33 NM + YMT + KMD	6.6	1.7	0.023 ± 0.003	8(6)
2000	18 Sep	31 NM	6.6	2.8	0.022 ± 0.005	11
2001	29 Aug	35 NM	15	7.4	0.03 ± 0.03	13
2003	31 Oct	37 NM + MUG	17.5	4.2	0.019 ± 0.006	13(7)
2004	12 Nov	35 NM + MUG	8.5	4.1	0.013 ± 0.004	12
2005	21 Jan[d]	36 NM + MUG + KMD	8.5	2.8	0.011 ± 0.005	6
2005	16 May	32 NM + MUG	7.8	4.8	0.017 ± 0.01	15(8)
2005	13 Sep	37 NM + MUG + KMD	11	4.1	0.026 ± 0.006	13
2006	15 Dec	33 NM + MUG	9	4.9	0.023 ± 0.007	12(6)

[a]The day of 7 May excluded from the analysis.
[b]The result is unstable.
[c]The day of 15 June excluded from the analysis.
[d]The day of 22 January excluded from the analysis.

the minimum phase (note that the CR cycle is inverted with respect to the sunspot cycle).

[13] We realize that these selection criteria may result in a certain bias of the analysis, since we consider only the recovery after the final event in the case of a series of transients. In this case, the recovery may in fact be affected by the previous disturbances. However, we believe that such a bias is hardly avoidable since more strict selection criteria will reduce the number of appropriate FDs and make a statistical study impossible.

2.2. Detector's Median Energy

[14] Following the usual approach [e.g., *Lockwood et al.*, 1991; *Lockwood and Webber*, 1996], we consider the characteristic energy of each detector to be the median energy E_M of its response function, with the following definition: the count rate of a cosmic ray detector (either NM or MT) can be expressed as [e.g., *Usoskin et al.*, 2005]

$$C = \int_{E_C}^{\infty} Y(E) \cdot S(E) \cdot dE, \quad (1)$$

where Y, S, and E denote the specific yield function of a detector, the differential energy spectrum of cosmic rays, and the primary particle's kinetic energy, respectively, and E_C is the energy, corresponding to the detector's local geomagnetic cutoff rigidity P_c. The median energy is then defined so that cosmic rays with energy above (or below) E_M contribute half to the detector's count rate, viz.

$$\int_{E_M}^{\infty} Y(E) \cdot S(E) \cdot dE = \int_{E_C}^{E_M} Y(E) \cdot S(E) \cdot dE = 0.5\, C, \quad (2)$$

Although this definition slightly depends on the phase of the solar cycle (the shape of $S(E)$) or the model used for $Y(E)$, the exact value of E_M is not important for this qualitative study. Here we use the following approximation for the median energy of a NM [see *Jämsén et al.* 2007, for full details]:

$$E_M = 0.0877 \cdot P_c^2 + 0.154 \cdot P_c + 10.12, \quad (3)$$

where E_M and P_c are expressed in GeV and GV, respectively. The median energy for the muon telescopes was computed directly by means of equation (2), using Monte-Carlo simulations of the detector's response. It was found to be 40 GeV for KMD and 55 GeV for YMT and MUG.

2.3. Forbush Decrease Recovery Phase

[15] The shape of the recovery phase can be roughly approximated by an exponential function with the characteristic recovery time, τ [*Webber*, 1962; *Lockwood et al.*, 1986]:

$$\delta I \equiv \frac{I_0 - I}{I_0} = M \cdot \exp\left(\frac{t_0 - t}{\tau}\right), \quad (4)$$

where I and I_0 are the current and undisturbed CR intensities, M is the magnitude of the FD, and t_0 is the beginning of the recovery phase. The magnitude M greatly varies from event to event reaching 25% for the strongest FDs on polar NMs. The value of M for the same event decreases from polar to equatorial stations as a function of the local geomagnetic rigidity cutoff of the detector, and thus depends on the energy of the CR. In the following analysis we define the best fit value of τ as the recovery time of a given FD observed at a given detector.

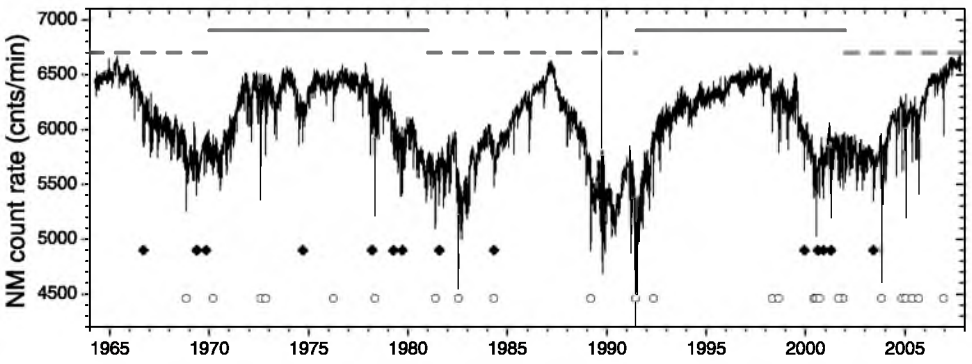

Figure 1. Count rate of Oulu NM for the entire period 1964–2007. Symbols denote Forbush decreases selected for the analysis, events of type I and II being marked by solid diamonds and open circles, respectively. Solid and dashed bars in the upper part denote the periods of the positive and negative polarity of the interplanetary magnetic field.

2.4. Analysis Method

[16] For each selected event, data from all available detectors were analyzed independently in the following steps.

[17] *Step 1 - Definition of the recovery time interval.* All available data are averaged over calendar days in order to exclude the diurnal variation which may be important, especially in the muon data. Then, the time interval for fitting the recovery phase is chosen to begin with the first full day after the main phase (shown in column 2 of Tables 2 and 3); this date is the same for all the detectors. The end of the fitting interval was varied to check the stability of the results, i.e., that the obtained recovery rate is not strongly dependent on the choice of the interval. If the results appear strongly dependent on the choice of the fitting interval, the corresponding event is rejected from further analysis. The length of the fit interval was the same for all NM data but may be shorter for MT data. In cases where a GLE occurred during the recovery phase, the entire day was removed from the analysis for all the detectors (see comments for Table 3). The selected intervals are listed in columns 7 and 9 of Tables 2 and 3.

[18] Major FDs can be accompanied by strong geomagnetic disturbances, which may slightly suppress the local geomagnetic cutoff of a detector for several hours [*Miyasaka et al.*, 2003; *Kudela and Brenkus*, 2004]. This may lead to a slight short distortion of the FD shape at midlatitude stations, while the effect is negligible for MTs and high-latitude NMs. However, in case of our statistical study it only leads to slightly larger uncertainties in the recovery time and do not affect the main result. Therefore we do not apply additional selection of the events with respect to the level of geomagnetic activity.

[19] *Step 2 - Computation of the individual recovery times.* The recovery phase was fit by an exponential recovery function equation (4) individually for each thus chosen fitting interval for FD (j) and for each detector (i) to provide the best fit values of M_{ji} and τ_{ji} (see examples in Figure 2). In order to check the stability of the results, the following boot-strap method was applied. From each data set I_{ji} we randomly removed two daily data points (or one if the fitting interval is shorter than 10 daily points) to produce a shorter data set I_{ji}^{*}, and this procedure is repeated 100 times. From 100 such shorter $\{I_{ji}^{*}\}$ data sets we compute a series of 100 values of $\{\tau_{ji}^{*}\}$ and $\{M_{ji}^{*}\}$, respectively. Then the mean and the standard deviation of the $\{\tau_{ji}^{*}\}$ were taken as estimates of the recovery rate τ_{ji} and its uncertainty $\sigma_{\tau,ji}$, respectively. Cases with $\sigma_{\tau,ji}$ exceeding τ_{ji} imply that the FD recovery profile is unstable, and the corresponding record was rejected from further analysis. The mean values of M_{ji} were obtained in

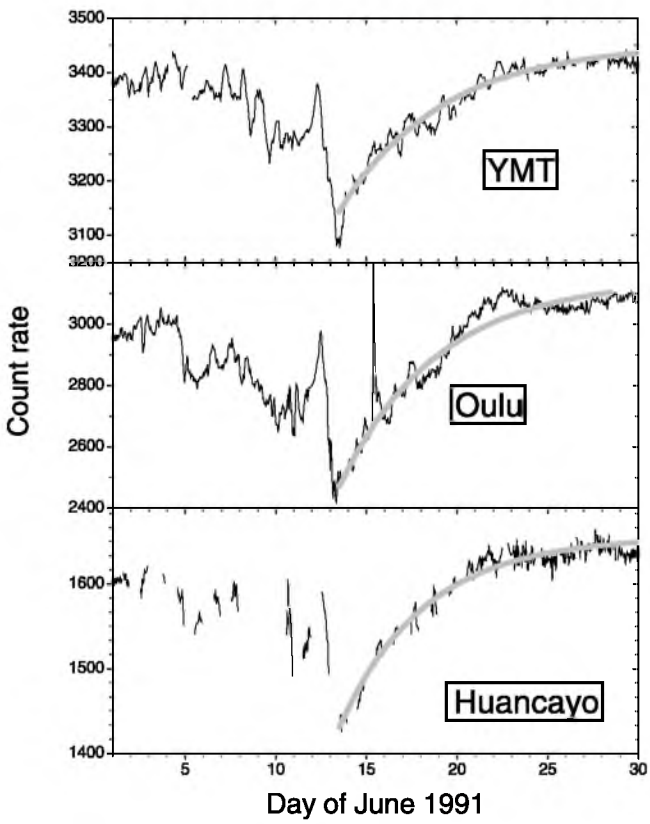

Figure 2. Count rates of YMT, Oulu NM and Huancayo NM (from top to bottom, respectively) for June 1991 together with the best fit exponential recovery (thick lines). The recovery time for YMT, Oulu and Huancayo are 6.7, 5.4, and 4.7 days, respectively.

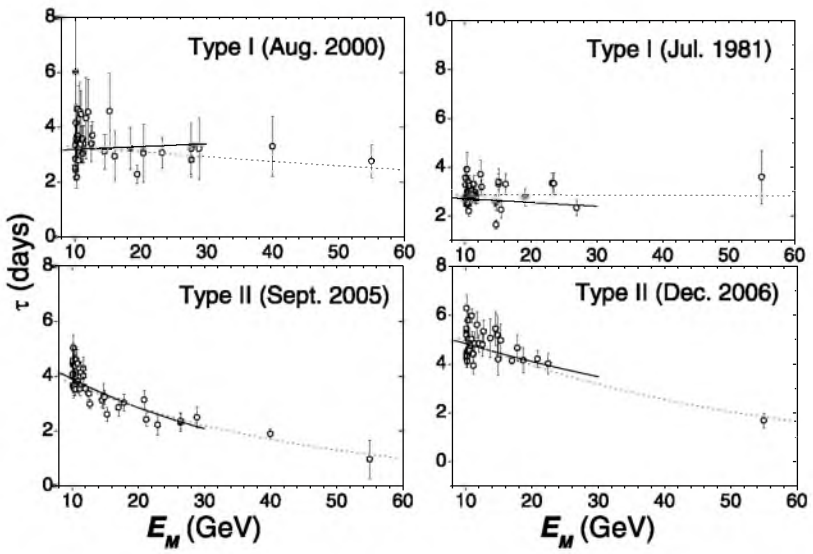

Figure 3. Examples of dependence of the recovery rate τ on the detector's median energy E_M (see text): Two events of Type I are plotted in the upper row, and two events of Type II in the lower row. Thin dotted and thick solid lines depict the best fit exponent functions (equation (5)) for all the data (NM + MT) and only NMs, respectively.

a similar way. Some examples of individual recovery times obtained in this way along with their uncertainties are shown in Figure 3 as a function of the detectors' median energy.

[20] *Step 3 – Analysis of the energy dependence.* Once the values of τ_{ji} have been obtained for j-th event and i-th detector, the relation τ_{ji}–vs–E_{Mj} was approximated by an exponential function:

$$\tau \propto \exp(-\alpha E_M), \tag{5}$$

where the value of α parameterizes the relation between the recovery time and the detector's median energy. The best fit parameter α together with its uncertainty σ_α of the relation (5) were computed using the standard least squares method applied to data with unequal accuracy. Examples of these relations are shown in Figure 3 as computed for NM data only (solid line) and for both NM and MT data (dotted). We note that the value of α has no clear physical meaning and only its sign is important for this study. Positive values of α imply an inverse energy dependence of the recovery time. The value of $\alpha \approx 0$ corresponds to no energy dependence of the recovery time. Significantly negative values of α would imply that the recovery time increase with energy but we have not found such cases. Finally, we formally assign one of two types to each j-th event.

[21] • Type I ($\alpha_j < \sigma_{\alpha,j}$) implies that there is no significant dependence of the recovery rate on energy (see upper panel in Figure 3);

[22] • Type II ($\alpha_j > \sigma_{\alpha,j}$) implies that the recovery rate does depend on energy (see lower panel in Figure 3).

[23] This division is formal and only aims for clearer analysis. In most cases, when MT data are available, the results based on only NM and both NM + MT are consistent with each other, except for the FD of March 1989 (marked as unstable in Table 3) which would be considered as a Type I event based on NM data only but appears to be a Type II event when both NM and YMT data are analyzed.

[24] *Step 4 – Mean parameters of FD.* For further analysis we also compute the parameters of the FD recovery phase, namely the mean magnitude $\langle M \rangle$ and recovery time $\langle \tau \rangle$ (depicted in columns 4 and 5, respectively). The values $\langle M \rangle$ and $\langle \tau \rangle$ were computed as the weighted mean over all high-latitude stations ($P_C < 1$ GV).

3. Results and Discussion

[25] The results of the analysis of the Forbush decrease recovery times are summarized in Tables 2 and 3. All 39 analyzed events can be divided in two groups – events of Type I (no clear energy dependence of the recovery time) and events of Type II (recovery time depends on the detector's median energy). We found 15 events of Type I and 24 events of Type II. First we note that the appearance of events of the two types is not related to the data-set used, therefore it is not biased by the use of MT data. The distribution of the events in time is shown in Figure 1. It is noteworthy that we did not find any apparent dependence of the occurrence of the events of a particular type on the IMF polarity (see Table 4). Both Type I and II events appear evenly (within the statistical uncertainties) for the positive and negative IMF polarities (Table 4).

Table 4. Dependence of the Occurrence of the Two Types of Events on the IMF Polarity

IMF Polarity	Events of Type I	Events of Type II
Negative (22 years)[a]	6	12
Positive (21 years)[a]	9	12

[a]Total duration of the periods of the corresponding IMF polarity in the analyzed time interval.

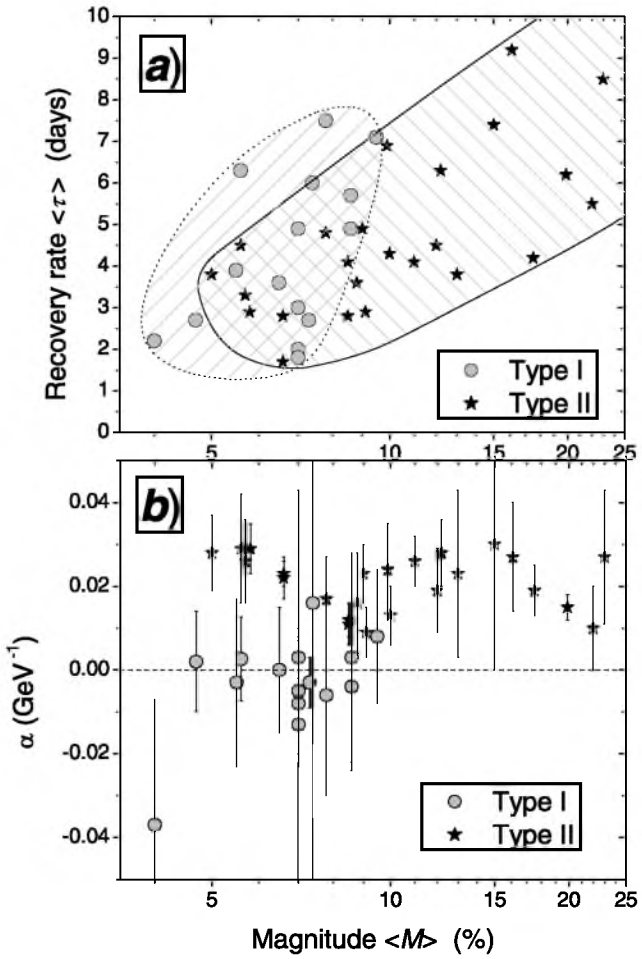

Figure 4. Results of the statistical analysis of FD recovery time. Grey dots and stars depict the results for type I (no energy dependence) and type II (significant energy dependence of the recovery time) events, respectively. Figure 4a shows the distribution of the events in the τ-vs-$\langle M \rangle$ plane, areas occupied by type I/II events are right/left-hand hatched and bounded by dotted/solid envelopes, respectively. Figure 4b shows the parameter α (see text for definition) as a function of the FD magnitude $\langle M \rangle$.

[26] The distribution of the two types of events in the $\langle M \rangle$-vs-$\langle \tau \rangle$ parametric space is shown in Figure 4a. All strong events with a mean magnitude $\langle M \rangle > 10\%$ fall into Type II, i.e., depict a clear energy dependence of the recovery time. Below a magnitude of 10% both types of events appear equally frequently. Additionally, the strength of the dependence (parameterized via the quantity α) is not related to the magnitude of the event, as apparent from Figure 4b. Although the parametric areas of their occurrence largely overlap, there is a small tendency that events of Type I have slightly slower recovery (larger $\langle \tau \rangle$) than those of Type II for the same magnitude $\langle M \rangle$.

[27] We do not claim here that Type I and Type II, formally analyzed here, provide a new classification for different kinds of FDs. Such a classification could be only made by studying each FD individually with all the parameters of the causing transient, which is beyond the scope of present study but planned for forthcoming studies. However, the present results do indicate that reduction of the recovery time with particle's energy is a real (beyond statistical doubts) phenomenon, which is often (but not always) observed.

[28] Since a Forbush decrease is caused by the passage of an interplanetary transient, the recovery phase is determined by the effect of dissipation of the shock modulation. This can occur in two different ways.

[29] *Radial departure of the shock*. As the shock moves further away from Earth, its effect on CR modulation at 1 AU weakens with heliocentric distance, leading to the gradual recovery of the cosmic ray intensity [e.g., *le Roux and Potgieter*, 1991]. According to models, such a process leads to little or no energy dependency of the recovery time, (which is mostly defined by the properties of the transient).

[30] *Longitudinal departure*. In concurrence with the radial departure of the shock, relative Sun-Earth geometry leads to the damping of the shock modulation effect. The transient, causing the FD, has a limited longitudinal extent. Accordingly due to the large relative solar rotational velocity (about 13.2 synodic degrees per day), our planet may run off the region, where IMF lines are connected to the shock. This can also lead to a recovery of the CR intensity. Moreover, when the edge of the longitudinal extent of the shock is approached, more energetic cosmic rays with larger gyroradii are expected to recover faster, thus leading to the energy dependence of the recovery rate. The characteristic time of the recovery in this case is defined by the longitudinal extent of the shock and the Earth's location relative to the shock during the main phase of the FD (whether it is near the center or eastern/western edge of the shock). The recovery time of 2–10 d corresponds to 30–150° in longitude, which gives reasonable values for the shock's longitudinal extent.

[31] In addition to these two mechanisms, which occur simultaneously, the CR transport in the third spatial dimension, namely latitudinal transport, can play a role in the CR recovery after a FD. Thus more sophisticated models, including 3D time-dependent modeling, are needed to understand the details of the CR transport in the inner heliosphere, and the results of this statistical study provide an empirical basis and constraint for such models.

[32] **Acknowledgments.** Anatoly Belov and Harm Moraal are gratefully acknowledged for stimulating discussions. Support from the Academy of Finland and the Finnish Academy of Science and Letters Vilho, Yrjö and Kalle Väisälä Foundation are acknowledged. We are grateful to the teams operating neutron monitors for their publicly available data used in this work.

[33] Amitava Bhattacharjee thanks the reviewers for their assistance in evaluating this paper.

References

Cane, H. V. (2000), Coronal mass ejections and Forbush decreases, *Space Sci. Rev.*, *93*, 55–77.

Jämsén, T., I. G. Usoskin, T. Räihä, J. Sarkamo, and G. A. Kovaltsov (2007), Case study of Forbush decreases: Energy dependence of the recovery, *Adv. Space Res.*, *40*, 342–347.

Kudela, K., and R. Brenkus (2004), Cosmic ray decreases and geomagnetic activity: List of events 1982–2002, *J. Atmos. Sol. Terr Phys.*, *66*, 1121–1126.

le Roux, J. A., and M. S. Potgieter (1991), The simulation of Forbush decreases with time-dependent cosmic ray modulation models of varying complexity, *Astron. Astrophys.*, *243*, 531–545.

Lockwood, J. A. (1960), An investigation of the Forbush decreases in cosmic radiation, *J. Geophys. Res.*, *65*, 3859–3880.

Lockwood, J. A., and W. R. Webber (1996), Comparison of the rigidity dependence of the 11-year cosmic ray variation at the earth in two solar cycles of opposite magnetic polarity, *J. Geophys. Res.*, *101*, 21,573–21,580.

Lockwood, J. A., W. R. Webber, and J. R. Jokipii (1986), Characteristic recovery times of Forbush-type decreases in the cosmic radiation: 1. Observations at Earth at different energies, *J. Geophys. Res.*, *91*, 2851–2857.

Lockwood, J. A., W. R. Webber, and H. Debrunner (1991), The rigidity dependence of Forbush decreases observed at the Earth, *J. Geophys. Res.*, *96*, 5447–5455.

Miyasaka, H., et al. (2003), Geomagnetic cutoff variation observed with TIBET Neutron Monitor, in *Proc. 28th Int. Cosmic Ray Conf.*, Tsukuba, Japan, *6*, 3609–3613.

Mulder, M. S., and H. Moraal (1986), The effect of gradient and curvature drift on cosmic-ray Forbush decreases, *Astrophys. J.*, *303*, L75–L78.

Östman, B. (1968), Studies of the recovery part of cosmic ray storms, *Ark. Geofys.*, *5*(25), 387–399.

Östman, B. (1969), The recovery rate and the energy dependence of decreases of the cosmic-ray intensity during the years 1957–1969, *Ark. Geofys.*, *6*, 549–568.

Penna, R. F., and A. C. Quillen (2005), Decay of interplanetary corona mass ejections and Forbush decrease recovery times, *J Geophys. Res.*, *110*, A09S05, doi:10.1029/2004JA010912.

Rana, D. S., N. K. Sharma, and R. S. Yadav (1996), The effect of gradient and curvature drifts on Forbush decreases, *Sol. Phys.*, *167*, 371–380.

Sandström, A. E., and S. E. Forbush (1958), Sudden decreases in cosmic-ray intensity at Huancayo, Peru, and at Uppsala, Sweden, *J. Geophys. Res.*, *63*(4), 876–878.

Singh, Y. P., and Badruddin (2006), Effects of the polarity states of the heliospheric magnetic field and particle drifts in cosmic radiation, *Sol. Phys.*, *234*, 339–352.

Usoskin, I. G., K. Alanko-Huotari, G. A. Kovaltsov, and K. Mursula (2005), Heliospheric modulation of cosmic rays: Monthly reconstruction for 1951–2004, *J. Geophys. Res.*, *110*, A12108, doi:10.1029/2005JA011250.

Webber, W. R. (1962), Time variations of low rigidity cosmic rays during the recent sunspot cycle, in *Progress in Elementary Particle and Cosmic Ray Physics*, edited by J. G. Wilson and S. A. Wouthuysen, North-Holland, Amsterdam, pp. 75–243.

Wibberenz, G., J. A. Le Roux, M. S. Potgieter, and J. W. Bieber (1998), Transient effects and disturbed conditions, *Space Sci. Rev.*, *83*, 309–348.

I. Braun, Max-Planck-Institut für Kernphysik, P.O. Box 103980, 69029 Heidelberg, Germany.

O. G. Gladysheva and G. A. Kovaltsov, Ioffe Physical-Technical Institute, Politekhnicheskaya 26, RU-194021 St. Petersburg, Russia.

J. R. Hörandel, Department of Astrophysics, Radboud University Nijmegen, P.O. Box 9010, 6500 GL Nijmegen, Netherlands.

T. Jämsén and I. G. Usoskin, Sodankylä Geophysical Observatory (Oulu Unit), University of Oulu, P.O. Box 3000, FIN-90014 Oulu, Finland. (ilya.usoskin@oulu.fi)

S. A. Starodubtsev, Yu.G. Shafer Institute of Cosmophysical Research and Aeronomy SB RAS, 31 Lenin Avenue, 677980 Yakutsk, Russia.